Title

Fruit fly scale robots can hover longer with flapping wings than with spinning wings

Journal

Journal of The Royal Society Interface, 13(123)

ISSN

1742-5689

Authors

Hawkes, Elliot W
Lentink, David

Publication Date

2016-10-01

DOI

10.1098/rsif.2016.0730

Peer reviewed

INTERFACE

rsif.royalsocietypublishing.org

Report

Cite this article: Hawkes EW, Lentink D. 2016 Fruit fly scale robots can hover longer with flapping wings than with spinning wings. *J. R. Soc. Interface* **13**: 20160730.
http://dx.doi.org/10.1098/rsif.2016.0730

Received: 8 September 2016
Accepted: 9 September 2016

Subject Category:
Life Sciences – Engineering interface

Subject Areas:
biomimetics

Keywords:
micro robot, hover, system performance, flapping wing, spinning wing, trade-off

Author for correspondence:
Elliot W. Hawkes
e-mail: ewhawkes@engineering.ucsb.edu

THE ROYAL SOCIETY
PUBLISHING

Fruit fly scale robots can hover longer with flapping wings than with spinning wings

Elliot W. Hawkes[1,2] and David Lentink[2]

[1]Department of Mechanical Engineering, University of California, Santa Barbara, CA 93106, USA
[2]Department of Mechanical Engineering, Stanford University, Stanford, CA 94305, USA

EWH, 0000-0002-0420-5025

Hovering flies generate exceptionally high lift, because their wings generate a stable leading edge vortex. Micro flying robots with a similar wing design can generate similar high lift by either flapping or spinning their wings. While it requires less power to spin a wing, the overall efficiency depends also on the actuator system driving the wing. Here, we present the first holistic analysis to calculate how long a fly-inspired micro robot can hover with flapping versus spinning wings across scales. We integrate aerodynamic data with data-driven scaling laws for actuator, electronics and mechanism performance from fruit fly to hummingbird scales. Our analysis finds that spinning wings driven by rotary actuators are superior for robots with wingspans similar to hummingbirds, yet flapping wings driven by oscillatory actuators are superior at fruit fly scale. This crossover is driven by the reduction in performance of rotary compared with oscillatory actuators at smaller scale. Our calculations emphasize that a systems-level analysis is essential for trading-off flapping versus spinning wings for micro flying robots.

1. Introduction

While manned flight has been optimized over the last century, a new aviation challenge has arisen at a much smaller scale—the scale of flying animals such as insects. The discovery that hovering insects can generate exceptionally high lift with a stable leading edge vortex [1,2], in combination with advances in micro electromechanical actuation and fabrication, has spurred the development of micro flying robots with flapping wings [3]. This innovation effort culminated in the wired take-off of the first bumblebee sized (approx. 30 mm wingspan) flapping robot [4]. The development of wireless bumblebee sized robots depends not only on new energy storage technologies; a critical advance is needed to make these micromechanical fliers more efficient so they require less power to hover [5]. Experiments with a dynamically scaled robotic fly wing show that spinning wings require less power than flapping wings to generate the same lift—from fruit fly (approx. 5 mm wingspan) to hummingbird (approx. 130 mm wingspan) scale [6]. Spinning wings also do not suffer from inertial losses; hence earlier studies concluded that flapping wings reduce the time a micro robot can hover in the air [7,8]. However, these studies only considered flapping wings driven by motors at the scale of hummingbirds and up; it is still unclear whether robots fly longer with wings flapped by piezos or spun with motors at hummingbird down to fruit fly scale [5]. The overall hover time of a micro flying robot depends on the efficiency of the actuator system that drives the wing [9], which has not yet been integrated in trade-off studies across scales.

Here, we reconcile existing analyses with a holistic system analysis to determine the hover time of micro robots with spinning versus flapping wings across scales. This analysis is focused on hover time without considering other performance metrics, such as payload capacity, controllability, manoeuvrability, flight speed or range. We integrated results from aerodynamic experiments with scaling

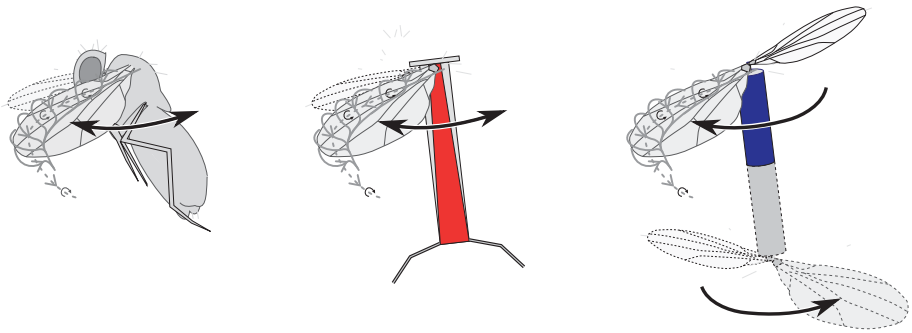

Figure 1. The finding that insects generate exceptionally high lift with a tornado-like leading edge vortex running spanwise along their wings [1,2], along with advances in micromechanical actuation and fabrication, inspired the development of insect scale robots with flapping wings [3]. Experiments with a dynamically scaled robot model of a hovering insect showed that micro robots can either flap or spin a *Drosophila*-like wing to generate a stable leading edge vortex to improve lift [6]. It is unclear which wing motion, flapping or spinning, is more energy efficient for large hummingbird down to fruit fly sized robots. (*Drosophila* cartoon modified from [6]; flapping robot from [4].) (Online version in colour.)

laws and data for performance of actuators, electronics and transmission mechanisms. According to this analysis, at fruit fly scales, robots should flap wings with oscillatory actuators to maximize hover time. By contrast, at hummingbird scale, robots should spin wings with rotary actuators. These results are largely driven by the scaling of actuator performance.

2. Hover duration of micro robots

Earlier studies either consider the energy consumption of the entire system at a single scale [7–12], qualitative performance differences at various scales [5], the performance of a flapping system across scales [13] or the aerodynamic power requirement of spinning versus flapping wings across scales [8]. For our holistic system analysis, we seek to determine how each parameter scales in the time of flight equation,

$$t_f = \frac{E_B}{P_{out}} \eta_a \eta_e \eta_m , \tag{2.1}$$

using the energy in the battery, E_B, divided by the output power needed to hover, P_{out} (comprising aerodynamic power, P_{aero}, and inertial power, P_{acc}), multiplied by the efficiencies of the actuators, η_a, electronics, η_e, and mechanical transmission mechanisms, η_m [9]. This data-driven scaling analysis enables us to compare the system performance of micro robots with wings that are spun by rotary actuators versus wings that are flapped by oscillatory actuators. Figure 1 shows representative sketches of such robots that use wings with leading edge vortices, as found in insects.

3. Integral hover time analyses across fruit fly to hummingbird scales

To predict the hover duration of a robot with fly-like wings that either spin or flap, we determine how the energy source, the battery and the energy sinks comprising aerodynamic power, inertial power and the losses in the actuators, electronics and transmission mechanisms scale. The electromechanical scaling laws are based on the function of the two main actuator technologies available for flying micro robots: the rotary electromagnetic motor, 'motor', for spinning wings and the oscillatory piezoelectric bimorph, 'piezo', for flapping wings (figure 1).

Our scaling analysis is based on the volumetric length scale, L, of the flier and determined by taking the cube root of flier mass, m, divided by its density (roughly 1000 kg m^{-3} for flying insects [14], hummingbirds [15] and flying robots [4,7,8]; based on reported robot mass and estimated volume). Critically, this volumetric length scale enables us to reconcile the scaling laws for the energy in the battery, E_B, the required aerodynamic power to fly, P_{aero}, the inertial power to flap, P_{acc}, and the efficiency of the actuators, η_a, electronics, η_e, and transmission mechanisms, η_m. The volumetric length scale, L, is, however, very different from the traditional wingspan scale, because the volumetric scale is associated with flier mass and independent of wing aspect ratio. The volumetric length scale associated with the published RoboFly measurements [6] that we use here are as follows: for fruit fly scale, mass is approximately 1 mg and L is approximately 1 mm; for bumblebee scale, mass is approximately 160 mg and L is approximately 5 mm; for hummingbird scale mass is approximately 16 g and L is approximately 25 mm. These volumetric length scales correspond to the following wingspans of approximately 5 mm, approximately 30 mm and approximately 130 mm, and are shown in figure 2*a* using corresponding animal cartoons for comparison.

We begin with the energy source, the battery, whose energy scales as the cube of the volumetric flier length scale. If we assume that available energy in the battery, E_B, is proportional to battery mass [11] and that battery mass is a fixed percentage of flier mass, then $E_B \propto L^3$. This energy is transformed in part into useful mechanical work that enables the flier to hover; the remainder is lost due to conversion inefficiencies and dissipated as heat.

A large portion of the energy from the battery is consumed by the aerodynamic power required to hover, which varies non-monotonically with volumetric length scale. The aerodynamic power, P_{aero}, is based on lift and drag measurements with a dynamically scaled robot fly model, with a robotically actuated wing, called 'RoboFly' [6] (figure 2*a*). RoboFly was used to determine the power needed to generate lift with flapping versus spinning fly wings across fruit fly, bumblebee and hummingbird scales [6]. Therefore, these measurements include all the Reynolds number, delayed stall, unsteady, rotational and other aerodynamic effects that enable insects to hover so well [1,2]. The published

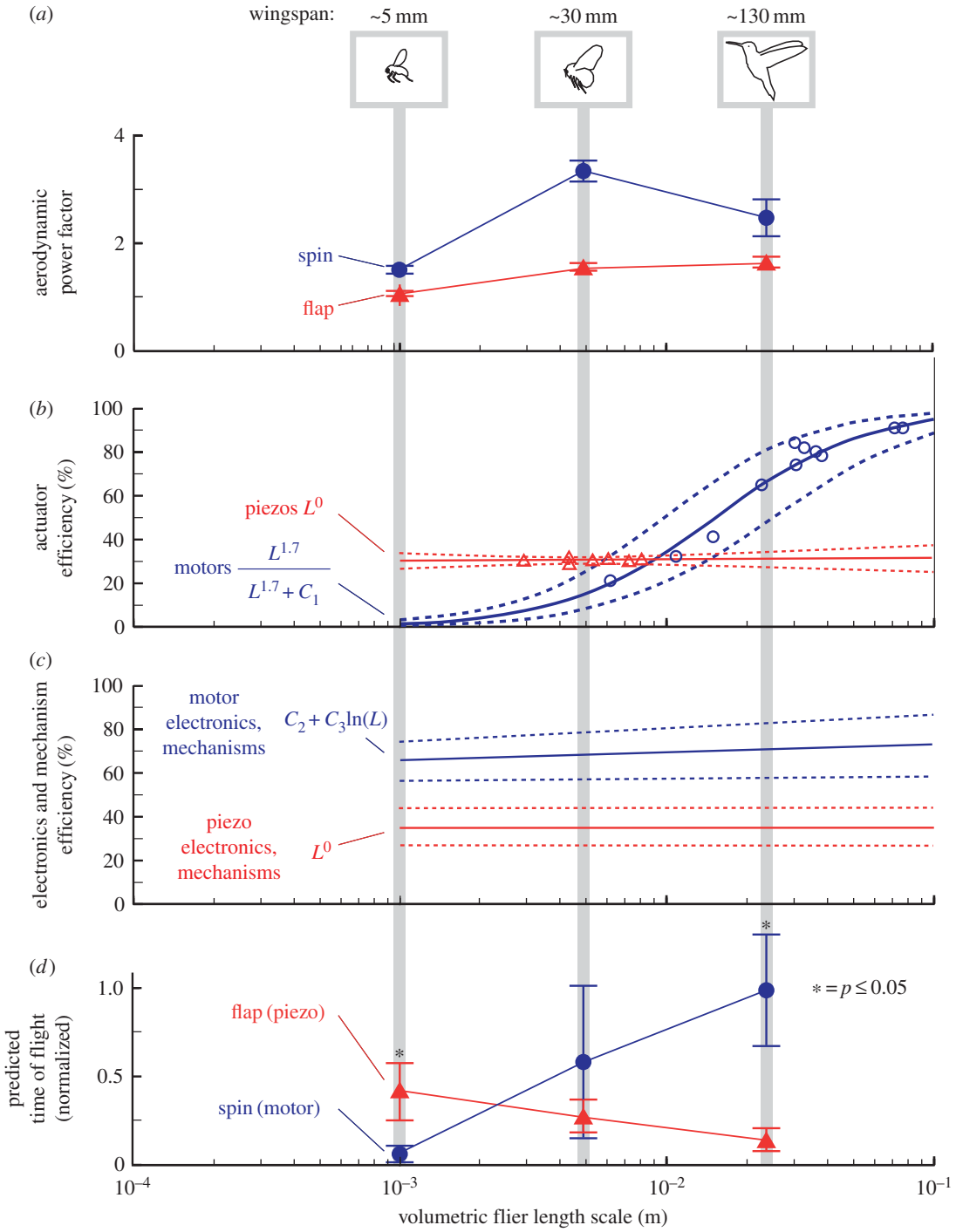

Figure 2. Scaling analysis explains why fruit fly scale robots hover longer with flapping wings driven by piezo actuators, while hummingbird scale robots hover longer with spinning wings powered by motors. In this scaling analysis, we reconcile both aerodynamic and electromechanical systems data based on the volumetric length scale, *L*, defined as the cube root of the quotient of flier mass and density. (*a*) The non-dimensional capacity of a *Drosophila*-like wing to lift weight with a unit of aerodynamic power (power factor) is highest when spun—from the scale of a fruit fly (mass: approx. 1 mg, *L*: approx. 1 mm) to a bumblebee (mass: approx. 160 mg, *L*: approx. 5 mm) and a large hummingbird (mass: approx. 16 g, *L*: approx. 25 mm) [6]. All recordings have been conducted with RoboFly placed in three different fluids (thick mineral oil, thin mineral oil, water) to match Reynolds number (110; 1400;14 000). Corresponding wingspans are given in mm for comparison. (*b*) Motor efficiency increases significantly at larger scales, while piezo efficiency is independent of scale. All motors are brushed except the smallest, which is brushless, the approximately 10% lower efficiency of the brushless controller is reconciled in this data point. The data points (motors [16,17], piezos [11,18]) are used to find the unknown parameters in the models using a least-squares fit. For piezos, we find an exponent of 0; for motors, we find an exponent of 1.7, and a constant, $C_1 = 0.001$. Dashed lines show 95% prediction intervals. The models are used to extrapolate motor performance for the fruit fly scale and piezo performance for the fruit fly and hummingbird scale. (*c*) The combined electronic and mechanical transmission efficiency of motor-driven spinning systems is weakly dependent on scale, whereas the efficiency for piezo-driven flapping systems is approximately independent of scale ($C_2 = 73$, $C_3 = 1.7$). (*d*) At hummingbird scale, micro robots with motor-driven spinning wings are more efficient than ones with piezo-driven flapping wings, and vice versa at fruit fly scale (significance level $p \leq 0.05$). Time of flight is normalized with the maximal calculated value at hummingbird scale. (Online version in colour.)

time-averaged non-dimensional 'power factor' values [6] are used to calculate the required time-averaged aerodynamic power to hover at every scale. Power factor, PF, is inverted and multiplied with a characteristic velocity, U_{ref} (based on Reynolds number), and weight, *W*: $P_{\text{aero}} = (1/PF)U_{\text{ref}}W$ [19]. For flapping wings, this calculation of aerodynamic power

holds for an actuator disc area corresponding to the stroke angle of fruit flies (140° [6]). We accounted for different actuator disc design trade-offs by considering the natural variation in stroke angle for eight common insects (stroke angle AVG: 127°, STD: 12° [20]). Based on this variation, we calculated the corresponding maximal variability in aerodynamic power due to differences in induced losses [20]. Further, the original RoboFly measurements were made with a rigid wing. While a flexible wing has been shown to increase aerodynamic efficiency for set angles of attack [21,22], a flexible wing was shown to not affect the maximum aerodynamic efficiency across angles of attack [23]. Therefore, the measurements from the rigid wing are suitable for our calculation. Also, the aerodynamic power for robots with spinning wings varies slightly depending on the configuration used to react the torque from the main rotor (a tail rotor increases required torque by AVG: 4%, STD: 2% [24], and a coaxial rotor configuration increases required torque by AVG: 3%, STD 2% [25], shown in figure 1). This variation is added to the uncertainty in the measurement of aerodynamic power. Aerodynamic power is, however, not the only sink of energy during hover, because flapping wings also have to overcome inertia during every wingbeat.

Flapping wings require additional inertial power, because they accelerate back and forth. The associated loss can be made small compared with aerodynamic power across scales if efficient elastic storage is used. This is explained as follows: acceleration can be powered by either a battery or elastic recoil,

$$P_{\mathrm{acc}} \propto I\dot{\Omega}\Omega, \tag{3.1}$$

to overcome the moment of inertia, I, of the flapping wing with angular acceleration, $\dot{\Omega}$, and angular velocity, Ω [19]. The inertial power scales with the length scale of the wing, L_{w}, to the power 3.5, because $I \propto L_{\mathrm{w}}^5$, and assuming isometry $\Omega \propto f \propto L_{\mathrm{w}}^{-0.5}$ [26] and as a result $\dot{\Omega} \propto f^2 \propto L_{\mathrm{w}}^{-1}$, thus $P_{\mathrm{acc}} \propto L_{\mathrm{w}}^{3.5}$. The aerodynamic power also scales with wing length to the power 3.5 under isometry, because $P_{\mathrm{aero}} \propto mfL_{\mathrm{w}} \propto L_{\mathrm{w}}^{3.5}$ [26]. Therefore, the relative contributions of P_{aero} and P_{acc} to P_{mech} do not change during isometric scaling of a given design. As flapping systems driven by spring-like piezos have been shown to have efficient elastic recoil at a 10 mm scale [27], we assume negligible P_{acc} across scales for this configuration. Beyond losses due to aerodynamic and inertial power, another set of losses arises from electromechanical inefficiencies.

The efficiency of motors decreases significantly at small scales, whereas the efficiency of piezos does not (figure 2*b*). This is explained by the actuator efficiency equation, $\eta_{\mathrm{a}} = P_{\mathrm{out}}/P_{\mathrm{in}}$, where $P_{\mathrm{in}} = P_{\mathrm{out}} + P_{\mathrm{loss}}$. For motors, P_{out} is modelled as scaling as $L^{3.5}$ [28] and

$$P_{\mathrm{loss}} = \frac{\tau^2}{K_{\mathrm{m}}^2} \quad \text{where} \quad K_{\mathrm{m}} \propto \sqrt{\frac{Nl^2B^2r^2}{R}} \tag{3.2}$$

with motor torque, τ, number of windings, N, length, l, field strength of the magnets, B, radius, r, and resistance, R [29]. This assumes the majority of losses are resistive [30]. As N, l, and r scale as L, B as L^0, and R as L^{-1}, K_{m} scales as L^3. Further, because τ scales as L^4 [31], P_{loss} then scales as L^8/L^6 or L^2. Therefore, the efficiency of motors theoretically scales as

$$\eta_{\mathrm{a,motor}} = \frac{L^{3.5}}{L^{3.5} + C_1L^2} = \frac{L^{1.5}}{L^{1.5} + C_1}, \tag{3.3}$$

where C_1 is a constant that relates the magnitudes of P_{out} and P_{loss} and can be determined from motor data. We corroborated equation (3.3) based on measured motor efficiencies using a least-squares fit of its general form and found the following exponents and coefficients: $\eta_{\mathrm{a,motor}} = L^{1.7}/(L^{1.7} + 0.001)$ (figure 2*b*), which we used in our scaling analysis. Data are from selected motors with relatively high efficiency across length scale. We created 95% confidence prediction intervals according to the methods described in [32] for the predicted values of efficiency at each scale (figure 2*b*). By contrast, the efficiency of piezos scales as L^0. This follows from the calculation of P_{out} as the product of force, $F \propto wt^2V/Lt$, deflection, $\delta \propto L_{\mathrm{c}}^2V/t^2$, and frequency, $f \propto t/L_{\mathrm{c}}^2$ [33]; with cantilever length, L_{c}, applied voltage, V, thickness, t, and width, w. L_{c}, t and w scale linearly with L. Thus $P_{\mathrm{out}} = F \cdot \delta \cdot f = wV^2/L$ and $P_{\mathrm{in}} = C_{\mathrm{b}}V^2f$, in which bimorph capacitance, C_{b}, scales as L using a parallel plate approximation [34]. Therefore, $\eta_{\mathrm{a,piezo}} = P_{\mathrm{out}}/P_{\mathrm{in}} = w/(LC_{\mathrm{b}}f)$, and because f scales as L^{-1} (above), $\eta_{\mathrm{a,piezo}} \propto L^0$. The efficiency for piezo bimorphs driven at resonance has been experimentally measured to be around 30% [27], and, in accordance with the prediction, is reported to scale as L^0 at this efficiency [35]. Our collected data confirm this trend (figure 2*b*) and include 95% prediction intervals. While losses due to the inefficiency of the actuators are substantial, there are additional inefficiencies associated with the electronics and the mechanical drivetrain.

Notable energy losses are found in the electronics and mechanisms, but, according to available data, these inefficiencies vary little across scale (figure 2*c*). For brushed motors, the electronic control efficiency is between 88% and 95% (AVG: 92%, STD: 3.5% [36,37]). Mechanism efficiency for a motor gearhead scales as $C_2 + C_3\ \ln(L)$, with constants C_2 and C_3 determined from gearhead data. This is because the losses are equal to an offset minus the natural logarithm of the gearhead reduction, r_{r}; $\ln(r_{\mathrm{r}})$ [38]. Then r_{r} scales as $L^{-0.5}$, because r_{r} is proportional to the ratio of motor angular velocity (L^{-1}; see above) and wing angular velocity ($L^{-0.5}$; see above). The gearhead losses are thus equal to $C_4 - C_5\ln(L^{-0.5})$, with constants C_4 and C_5. Efficiency is then $1 - \text{loss} = C_2 + C_3\ln(L)$. By contrast, piezos require high voltages and existing boost converters to generate these voltages are roughly 70% efficient (AVG: 68%, STD: 9% [34]), provided they are used at optimal power output. Further, existing high voltage drive electronics are roughly 50% efficient (AVG: 53%, STD: 2% [34]). Piezos use a transmission mechanism to amplify the small motion of the actuator, and, if a linkage mechanism with flexures as joints is used [27], the efficiency is high and varies slightly due to manufacturing tolerances (AVG: 90%, STD: 8% [27]).

Finally, we determined the hover time for fruit fly to hummingbird scales by integrating the scaling of the above energy sources and sinks into the time of flight equation (equation (2.1)). Next, we determined the corresponding 95% prediction intervals, by propagating the uncertainty in each of the terms in equation (2.1), to see if this modifies our hover time conclusions (figure 2*d*). This data-driven scaling analysis predicts that wings flapped by a piezo actuator result in longer hover time at the scale of a fruit fly (significance level $p \leq 0.05$). By contrast, our model suggests the hover time for wings spun by a motor is greater at the scales of a hummingbird ($p \leq 0.05$). This result is robust for remarkably low piezo efficiencies down to about 7%, suggesting that more damping at smaller scales can be overcome.

4. Actuator performance drives flapping versus spinning design trade-off

Our holistic scaling analysis shows that fruit fly sized robots can hover longer with flapping wings actuated by piezo actuators, because the lower aerodynamic efficiency of flapping wings is compensated by the higher efficiency of piezo actuators. Hummingbird sized robots, however, can hover much longer with motor-driven spinning wings, because of combined high aerodynamic and electromechanical efficiencies. This crossover in micro robot design optima is driven by how the performance of current actuator technology scales. Our analysis suggests that future fruit fly sized robots might hover longer if a new piezo-driven transmission mechanism would be developed to spin wings. Such futuristic piezo-driven microcopters would marry the best aerodynamic and actuator efficiencies currently available at the micro-aviation frontier.

Authors' contributions. E.W.H. conceived the study, E.W.H. and D.L. derived models and wrote the manuscript. Both authors gave final approval for publication.

Competing interests. We have no competing interests.

Funding. No funding has been received for this article.

Acknowledgements. We thank Michael Karpelson for helpful discussions on piezos. We thank Eric Eason for helpful discussions on statistics.

References

1. Ellington CP, Van Den Berg C, Willmott AP, Thomas ALR. 1996 Leading-edge vortices in insect flight. *Nature* **384**, 626–630. (doi:10.1038/384626a0)
2. Dickinson MH, Lehmann FO, Sane SP. 1999 Wing rotation and the aerodynamic basis of insect flight. *Science* **284**, 1954–1960. (doi:10.1126/science.284.5422.1954)
3. Lentink D. 2013 Biomimetics: flying like a fly. *Nature* **498**, 306–307. (doi:10.1038/nature12258)
4. Ma KY, Chirarattananon P, Fuller SB, Wood RJ. 2013 Controlled flight of a biologically inspired, insect-scale robot. *Science* **340**, 603–607. (doi:10.1126/science.1231806)
5. Floreano D, Wood RJ. 2015 Science, technology and the future of small autonomous drones. *Nature* **521**, 460–466. (doi:10.1038/nature14542)
6. Lentink D, Dickinson MH. 2009 Rotational accelerations stabilize leading edge vortices on revolving fly wings. *J. Exp. Biol.* **212**, 2705–2719. (doi:10.1242/jeb.022269)
7. Keennon M, Klingebiel K, Won H, Andriukov A. 2012 Development of the nano hummingbird: a tailless flapping wing micro air vehicle. In *Proc. 50th AIAA Aerospace Sciences Meeting including the New Horizons Forum and Aerospace Exposition, Nashville, TN, 9–12 January 2012*, pp. 9–12. Reston, VA: American Institute of Aeronautics and Astronautics.
8. Lentink D, Jongerius SR, Bradshaw NL. 2010 The scalable design of flapping micro-air vehicles inspired by insect flight. In *Flying insects and robots*, pp. 185–205. Berlin, Germany: Springer.
9. Karpelson M, Whitney JP, Wei GY, Wood RJ. 2010 Energetics of flapping-wing robotic insects: towards autonomous hovering flight. In *Proc. IEEE/RSJ Int. Conf. on Intelligent Robots and Systems* (*IROS*), *Taipei, Taiwan, 18–22 October 2010*, pp. 1630–1637. New York, NY: IEEE.
10. Bohorquez F, Samuel P, Sirohi J, Pines D, Rudd L, Perel R. 2003 Design, analysis and hover performance of a rotary wing micro air vehicle. *J. Am. Helicopter Soc.* **48**, 80–90. (doi:10.4050/JAHS.48.80)
11. Karpelson M, Wei GY, Wood RJ. 2008 A review of actuation and power electronics options for flapping-wing robotic insects. In *Proc. IEEE Int. Conf. on Robotics and Automation* (*ICRA 2008*), *Pasadena, CA, 19–23 May 2008*, pp. 779–786. New York, NY: IEEE.
12. Abdilla A, Richards A, Burrow S. 2015 Endurance optimisation of battery-powered rotorcraft. In *Towards autonomous robotic systems*, pp. 1–12. Berlin, Germany: Springer.
13. Whitney JP, Wood RJ. 2012 Conceptual design of flapping-wing micro air vehicles. *Bioinspir. Biomim.* **7**, 036001. (doi:10.1088/1748-3182/7/3/036001)
14. Moya-Laraño J, Macías-Ordóñez R, Blanckenhorn WU, Fernández-Montraveta C. 2008 Analysing body condition: mass, volume or density? *J. Anim. Ecol.* **77**, 1099–1108. (doi:10.1111/j.1365-2656.2008.01433.x)
15. Carpenter FL, Hixon MA, Beuchat CA, Russell RW, Paton DC. 1993 Biphasic mass gain in migrant hummingbirds: body composition changes, torpor, and ecological significance. *Ecology* **74**, 1173–1182. (doi:10.2307/1940487)
16. Faulhaber F. 2012 *Miniature drive systems*. Schonaich, Germany: Faulhaber GMBH.
17. Precision Microdrives Limited (PML). 2015 *NanoCore Datasheet*. London, UK: Precision Microdrives Limited.
18. Steltz E, Fearing RS. 2009 Dynamometer power output measurements of miniature piezoelectric actuators. *IEEE/ASME Trans. Mech.* **14**, 1–10. (doi:10.1109/TMECH.2008.2005902)
19. Wang ZJ. 2008 Aerodynamic efficiency of flapping flight: analysis of a two-stroke model. *J. Exp. Biol.* **211**, 234–238. (doi:10.1242/jeb.013797)
20. Nabawy MRA, Crowther WJ. 2014 On the quasi-steady aerodynamics of normal hovering flight part I: the induced power factor. *J. R. Soc. Interface* **11**, 20131196. (doi:10.1098/rsif.2013.1196)
21. Young J, Walker SM, Bomphrey RJ, Taylor GK, Thomas AL. 2009 Details of insect wing design and deformation enhance aerodynamic function and flight efficiency. *Science* **325**, 1549–1552. (doi:10.1126/science.1175928)
22. Kang CK, Aono H, Cesnik CE, Shyy W. 2011 Effects of flexibility on the aerodynamic performance of flapping wings. *J. Fluid Mech.* **689**, 32–74. (doi:10.1017/jfm.2011.428)
23. Zhao L, Huang Q, Deng X, Sane SP. 2010 Aerodynamic effects of flexibility in flapping wings. *J. R. Soc. Interface* **7**, 485–497. (doi:10.1098/rsif.2009.0200)
24. Leishman JG. 2006 *Principles of helicopter aerodynamics*. Cambridge, UK: Cambridge University Press.
25. Bohorquez F. 2007 Rotor hover performance and system design of an efficient coaxial rotary wing micro air vehicle. PhD dissertation, University of Maryland, College Park, MD, USA, pp. 186–192.
26. Norberg UM. 2012 *Vertebrate flight: mechanics, physiology, morphology, ecology and evolution*, pp. 166–179. Berlin, Germany: Springer.
27. Steltz E, Seeman M, Avadhanula S, Fearing RS. 2006 Power electronics design choice for piezoelectric microrobots. In *Proc. IEEE/RSJ Int. Conf. on Intelligent Robots and Systems, Beijing, China, 9–15 October 2006*, pp. 1322–1328. New York, NY: IEEE.
28. Ghosh A. 2011 Scaling laws. In *Mechanics over micro and nano scales*, pp. 61–94. New York, NY: Springer.
29. Seok S, Wang A, Otten D, Kim S. 2012 Actuator design for high force proprioceptive control in fast legged locomotion. In *Proc. IEEE/RSJ Int. Conf. on Intelligent Robots and Systems* (*IROS*), *Vilamoura-Algarye, Portugal, 7–12 October 2012*, pp. 1970–1975. New York, NY: IEEE.
30. Emadi A. 2004 *Energy-efficient electric motors, revised and expanded*. Boca Raton, FL: CRC Press.
31. Chatzakos P, Papadopoulos E. 2008 The influence of DC electric drives on sizing quadruped robots. In *Proc. IEEE Int. Conf. on Robotics and Automation* (*ICRA 2008*), *Pasadena, CA, 19–23 May 2008*, pp. 793–798. New York, NY: IEEE.
32. Montgomery DC, Runger GC. 2011 *Applied statistics and probability for engineers*, 5th edn. New York, NY: Wiley.
33. Wang QM, Cross LE. 1998 Performance analysis of piezoelectric cantilever bending actuators. *Ferroelectrics* **215**, 187–213. (doi:10.1080/00150199808229562)
34. Karpelson M, Wei G-Y, Wood R. 2012 Driving high voltage piezoelectric actuators in microrobotic applications. *Sensors Actuators A Phys.* **176**, 78–89. (doi:10.1016/j.sna.2011.11.035)

35. Uchino K. 2008 Piezoelectric actuators 2006. *J. Electroceramics* **20**, 301–311. (doi:10.1007/s10832-007-9196-1)
36. Noth A, Siegwart R. 2010 Solar-powered micro-air vehicles and challenges in downscaling. In *Flying insects and robots*, pp. 285–297. Berlin, Germany: Springer.
37. Harrington A, Kroninger C. 2013 Characterization of small dc brushed and brushless motors. Report no. ARL-TR-6389. Army Research Laboratory, Aberdeen Proving Ground Vehicle Technology Directorate, MD, USA.
38. Faulhaber F. 2002 *A second look at gearbox efficiencies*. See http://machinedesign.com/archive/second-look-gearbox-efficiencies.